

of the metal with the cationic ligand compared to the neutral xylene homologue, this difference in reactivity is yet another manifestation of the importance of back-bonding in the chemistry of Os(II) centers.

Conclusion

The existence of stable η^2 complexes of pentaammineosmium(II) with poor σ donors such as the above-mentioned cationic heterocycles is remarkable. The interaction of Os(II) with protic ligands such as pyridinium ion is even more striking, given the highly reducing properties of the pentaammineosmium(II) moiety, which render it unstable with respect to oxidation in the presence of protons, and must be a reflection of the high affinity of this electron-rich metal for unsaturated centers.

Reports on η^2 -bound nitrogen aromatic heterocycles are scarce. The few reported cases feature coordinatively unsaturated metals

with N,C-bound ligands that either are formally doubly reduced²² or have lost an ortho proton²³ and hence differ markedly from the free ligands. The present work on pentaammineosmium(II) thus represents a unique example of metal π coordination to nitrogen heterocycles. Furthermore, it provides a useful model in the study of aromatic C-H bond activation by transition metals.

Acknowledgment. We thank the National Institutes of Health (Grant GMI3638-22) and the National Science Foundation (Grant CHE84-14329) (400-MHz NMR) for support of this work.

(22) Neithamer, D. R.; Pärkányi, L.; Mitchell, J. F.; Wolczanski, P. T. *J. Am. Chem. Soc.* **1988**, *110*, 4421.

(23) Thompson, M. E.; Baxter, S. M.; Bulls, A. R.; Burger, B. J.; Nolan, M. C.; Santarsiero, B. D.; Shaefer, W. P.; Bercaw, J. E. *J. Am. Chem. Soc.* **1987**, *109*, 203.

Regioselective Oxidation Catalysis in Synthetic Phospholipid Vesicles. Membrane-Spanning Steroidal Metalloporphyrins

John T. Groves* and Ronny Neumann†

Contribution from the Department of Chemistry, Princeton University, Princeton, New Jersey 08544. Received August 22, 1988

Abstract: A membrane-spanning porphyrin has been synthesized by attaching four 3β -hydroxy-5-cholenic acid moieties to $\alpha,\beta,\alpha,\beta$ -meso-tetrakis(*o*-aminophenyl)porphyrin. The resulting steroidal porphyrin, H₂ChP, and the corresponding metalloporphyrins, MChP, were shown by gel permeation chromatography, ³¹P NMR, and differential scanning calorimetry to intercalate into vesicle bilayers. The steroidal porphyrin was found to be in a well-defined and highly ordered microenvironment within the bilayer. The anisotropic ESR spectra of Cu^{II}(ChP) in orientated bilayer assemblies on Mylar film clearly indicated that the plane of the porphyrin ring was parallel to the plane defined by the bilayer-water interface. The porphyrin ring was also found to be in the middle of the bilayer with fluctuations of ± 3 -4 Å around the center. This was shown by use of tethered imidazole ligands of the general formula Im(CH₂)_nCOOH as molecular probes. Ligation to Co^{II}(ChP) could be monitored by ESR as a function of the length of the tethered ligand and conclusively demonstrated that only ligands where $n > 6$ were able to coordinate to the metal. Iron(III) and manganese(III) steroidal porphyrins were then used as regioselective epoxidation and hydroxylation catalysts. Diolefinic sterols were epoxidized exclusively at the side chain. Epoxidation of polyunsaturated fatty acids was preferred by a ratio of 2/1 at the more hydrophobic terminus and it was found that by increasing the rigidity of the bilayer by the addition of cholesterol the selectivity could be raised to 9/1. Finally, it was shown that cholesterol could be selectively hydroxylated at the C₂₅ tertiary carbon.

Major efforts have been made in recent years to formulate regioselective and stereoselective catalytic systems. The importance of such systems is borne out by the significant impact made by processes such as shape-selective catalysis by zeolites¹ and homogeneous chiral hydrogenations² and catalytic asymmetric oxidations.³ Among the many diverse catalytic systems investigated, those mimicking enzymatic biocatalysis have attracted particular attention. The development of synthetic chemical models that mimic the active site of heme proteins has afforded a detailed understanding of the oxygen binding by globins⁴ and oxidations mediated by cytochrome P-450.⁵ The binding or arrangement of a potentially reactive substrate in a spatially selective manner so that only a certain defined reaction pathway is possible is another important aspect of enzyme catalysis. The guest-host interactions of crown ethers,⁶ cyclodextrins,⁷ and molecular clefts⁸ have been used extensively to mimic selective binding. Intramolecular geometric control of reactions has also been achieved by appending carefully designed reactive reagents to target substrates.⁹ Finally, the intrinsic molecular order found

in the microenvironments of monolayers, micelles,¹⁰ and vesicle bilayers¹¹ has been used with more limited success to specially

(1) Whyte, T. E.; Dalla Betta, R. A. *Catal. Rev.-Sci. Eng.* **1982**, *24*, 567 and references therein.

(2) (a) Morrison, J. D.; Masler, W. F.; Neuberger, M. K. *Adv. Catal.* **1976**, *25*, 81. (b) Brown, J. M.; Cholener, P. A.; Murrer, B. A.; Parker, D. *ACS Symp. Ser.* **1980**, *119*, 169. (c) Halpern, J. In *Asymmetric Synthesis*; Morrison, J. D., Ed.; Academic: New York, 1985; Vol. 5, p 41.

(3) (a) Katsuki, T.; Sharpless, K. B. *J. Am. Chem. Soc.* **1980**, *102*, 5974. (b) Rossiter, B. E.; Katsuki, T.; Sharpless, K. B. *J. Am. Chem. Soc.* **1982**, *103*, 464. (c) Rossiter, B. E. In *Asymmetric Synthesis*; Morrison, J. D., Ed.; Academic: New York, 1985; Vol. 5, p 194.

(4) Traylor, T. J.; Koga, N.; Deardurff, L. A. *J. Am. Chem. Soc.* **1985**, *107*, 6504 and references therein.

(5) Ortiz de Montellano, P. *Cytochrome P-450*; Plenum: New York, 1986.

(6) Stoddart, J. F. *New Compr. Biochem.* **1984**, *6*, 529.

(7) (a) Bender, M. L.; Komiyama, M. *Cyclodextrin Chemistry*; Springer: New York, 1978. (b) Tabushi, I.; Kuroda, Y. *Adv. Catal.* **1983**, *32*, 417. (c) Breslow, R. In *Inclusion Compounds*; Atwood, J. L., Davies, J. E. D., MacNicol, D. D., Eds.; Academic: New York, 1984; Vol. 3, p 473.

(8) (a) Rebek, J.; Askew, B.; Killoran, M.; Nemeth, D.; Lin, F.-T. *J. Am. Chem. Soc.* **1987**, *109*, 2426. (b) Rebek, J.; Askew, B.; Nemeth, D.; Parris, K. *J. Am. Chem. Soc.* **1987**, *109*, 2432.

(9) Breslow, R. *Acc. Chem. Res.* **1980**, *13*, 170.

(10) Fendler, J. H. *Membrane Mimetic Chemistry*; Wiley: New York, 1982.

* Author to whom correspondence should be addressed.

† Current address: Casali Institute of Applied Chemistry, The Hebrew University of Jerusalem, Israel.

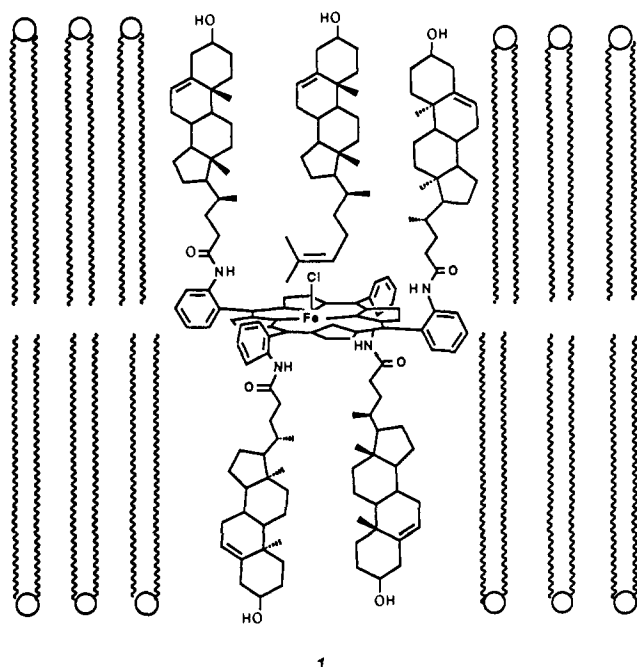


Figure 1. Idealized drawing of molecular bilayer assembly of chloro- $[\alpha,\beta,\alpha,\beta\text{-}meso\text{-tetrakis}[o\text{-}((3\beta\text{-hydroxy-5-cholenyl)amido})phenyl]\text{-porphyrinato}]iron(III)$ ($Fe^{III}(\text{ChP})\text{Cl}$), desmosterol, and phospholipid.

arrange substrates so that regioselective reactivity may be induced.

In this paper we describe the synthesis of a porphyrin with two steroid moieties appended from either side of the porphyrin plane. The pillared shape of this steroidal porphyrin has molecular dimensions complementary to the width of a synthetic phospholipid bilayer membrane. Accordingly, intercalation of this steroidal porphyrin into a phosphocholine bilayer could produce a site-selective catalytic assembly. We have recently reported selective epoxidation on the side chain of diolefinic steroids, the epoxidation at the hydrophobic terminus of polyunsaturated fatty acids.¹² The selective C_{25} hydroxylation of cholesterol has also been achieved. The porphyrin-bilayer assembly as drawn in Figure 1 implies a well-defined and highly ordered microenvironment within the bilayer. Specifically, it has been assumed on the basis of the synthetic design and observed selectivities that the porphyrin ring is perpendicular to the bilayer normal and rigidly centered between the two layers. Experiments using ESR as a spectral probe have now verified these premises. The preparation of an oriented bilayer assembly on a spectrally silent Mylar film has afforded anisotropic ESR spectra, which confirm the relative orientation of the porphyrin ring and the phospholipid bilayer. The use of specifically synthesized amphiphilic imidazole ligands has confirmed that the porphyrin is centered in the bilayer with fluctuations of only 3–4 Å.

Results and Discussion

Synthesis. The membrane-spanning porphyrin (**1**) was synthesized by attaching four 3β -hydroxy-5-cholenic acid residues to the $\alpha,\beta,\alpha,\beta$ atropisomer of *meso*-tetrakis(*o*-aminophenyl)-porphyrin by forming amide bonds. The complete reaction scheme (Figure 2) involves first the protection of the alcohol group of the cholenic acid by way of formation of a formate ester. A mixed anhydride of the cholenic acid was then formed with isobutylchloroformate in dry THF with triethylamine as acid scavenger. Afterward the mixed anhydride was condensed with $\alpha,\beta,\alpha,\beta\text{-}meso\text{-tetrakis}(o\text{-aminophenyl})porphyrin$ using 4-(dimethyl-

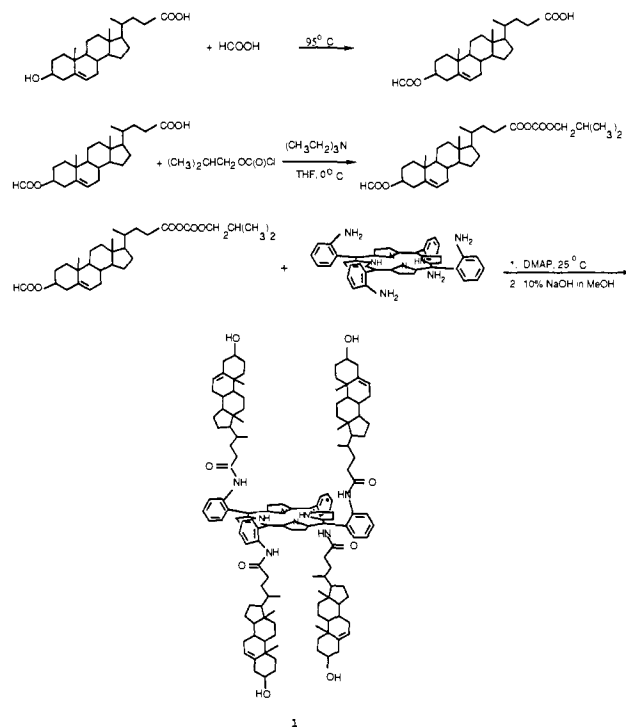


Figure 2. Reaction scheme for the synthesis of $\alpha,\beta,\alpha,\beta\text{-}meso\text{-tetrakis}[o\text{-}((3\beta\text{-hydroxy-5-cholenyl)amido})phenyl]porphyrin$, $H_2\text{ChP}$.

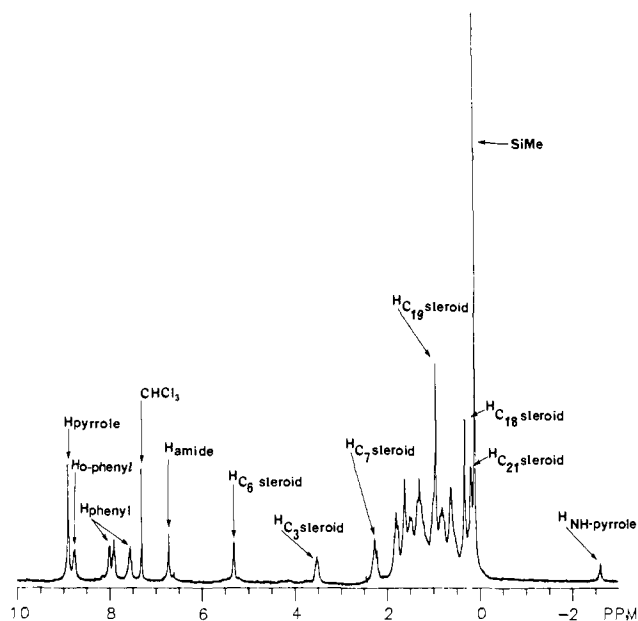


Figure 3. ^1H NMR of $\alpha,\beta,\alpha,\beta\text{-}meso\text{-tetrakis}[o\text{-}((3\beta\text{-hydroxy-5-cholenyl)amido})phenyl]porphyrin$ in CDCl_3 at 300 MHz.

amino)pyridine as a nucleophilic catalyst. The product, tetrakis(*o*-cholenylamidophenyl)porphyrin, [$H_2(\text{ChP})$] (**1**), was purified by column chromatography after deprotection of the formate ester moiety with basic methanol. The steroidal porphyrin was characterized by both its ^1H NMR spectrum (Figure 3) and its FAB mass spectrum (Figure 4). The ^1H NMR spectrum shows characteristics of both the tetraphenylporphyrin and steroid moieties. The tetraphenylporphyrin portion of the molecule contributes a singlet at δ 8.88 for the β -pyrrole hydrogens confirming the $\alpha,\beta,\alpha,\beta$ configuration. Other configurations (except the highly unlikely $\alpha,\alpha,\alpha,\alpha$) or a steroid appendage-porphyrin ring ratio not equal to 4 would not have given a pyrrole singlet. At δ 8.74 one finds a doublet attributable to the phenyl hydrogens ortho to the porphyrin group. The remaining phenyl hydrogens are seen as two triplets and a doublet at fields between δ 8.0 and

(11) (a) Czarniecki, M. F.; Breslow, R. *J. Am. Chem. Soc.* **1979**, *101*, 3675. (b) Moss, R. A.; Schreck, R. P. *J. Am. Chem. Soc.* **1985**, *107*, 6634 and references therein. (c) van Easch, J.; Roks, M. F. M.; Nolte, R. J. M. *J. Am. Chem. Soc.* **1986**, *108*, 6093. (d) Fuhrhop, J.-H.; Matieu, J. *Angew. Chem., Int. Ed. Engl.* **1984**, *23*, 100.

(12) Groves, J. T.; Neumann, R. *J. Am. Chem. Soc.* **1987**, *109*, 5045.

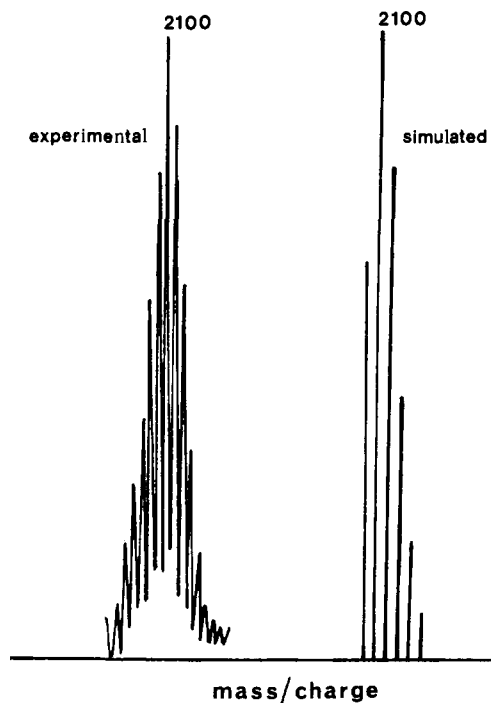


Figure 4. Experimental and simulated molecular ion cluster in the FABMS of $\alpha,\beta,\alpha,\beta$ -*meso*-tetrakis[*o*-((3 β -hydroxy-5-cholenoyl)amido)phenyl]porphyrin.

7.5. The amido hydrogen appears at δ 6.70 as a singlet, and the NH pyrrole singlet is found at δ -2.64. The steroid moiety can be clearly identified by the typical peaks of the vinylic C₆ hydrogen, the C₃ hydrogen adjacent to the hydroxyl group, the allylic C₇ hydrogens, and the C₁₉, C₁₈, and C₂₁ methyl groups. There is a significant upfield shift of the C₂₁ (δ 0.31 vs 0.96) hydrogen resonance compared to that of 3 β -hydroxy-5-cholenic acid due to the proximity and position above the porphyrin ring. The ratio of four steroid groups per porphyrin ring was indicated by the β -pyrrole singlet and confirmed by integration. Further confirmation of the molecular weight was derived from the FABMS (Figure 4). The spectrum (from a *m*-nitrobenzyl alcohol matrix) shows a molecular ion cluster at the expected m/z 2100. Comparison of the molecular ion cluster of the actual spectrum with the simulated spectrum showed very good correlation. The experimental cluster also indicated a significant abundance of $M^+ - 1$, $M^+ - 2$, etc., ions due to fragments formed upon loss of hydrogen. No ions were found at m/z values that could be attributed to a porphyrin with less than four steroid appendages.

The porphyrin was metalated in the usual manner giving iron(III), manganese(III), copper(II), and cobalt(II) metalloporphyrins, which were identified by their visible spectra and FABMS (Table I). The steroidal porphyrins thus formed have a total hydrophobic length complementary to a dimyristoylphosphocholine (DMPC) or a dipalmitoylphosphocholine (DPPC) bilayer (35–40 Å). The equatorial C₃ hydroxyl groups of the steroid appendages are arranged so that they may interact with the aqueous phases on either side of a bilayer membrane (Figure 1). Ideally, the heme ring of the H₂(ChP) porphyrin would be centered in the bilayer and perpendicular to the bilayer normal.

Vesicle Characterization. Preliminary characterization indicated that a mixture of steroid porphyrin and DMPC indeed formed a normal vesicular system. Small unilamellar vesicles were prepared by the method of ultrasonication of thin films of phospholipid and porphyrin.¹³ Phospholipid and the steroidal porphyrin (**1**) were dissolved in a minimum amount of chloroform in a test tube. The solvent was evaporated under a stream of nitrogen, leaving a thin film, and aqueous phase was added. The mixture was sonicated with an immersed microtip for ca. 5 min

Table I. Visible and FAB Mass Spectra of Steroidal Porphyrins

steroidal porphyrin	visible spectrum: λ_{\max} (log ϵ)	FABMS, m/z (intensity, %)
H ₂ (ChP)	422 (5.40), 516 (4.09), 549 (3.54), 590 (3.60), 645 (3.30)	2099 (78), 2100 (100), 2101 (86), 2102 (59), 2103 (32), 2104 (17)
Fe ^{III} (ChP)Cl	420 (4.83), 510 (3.94), 584 (3.68), 654 (3.20)	2154 (85), 2155 (100), 2156 (89), 2157 (58), 2158 (40), 2159 (25)
Mn ^{III} (ChP)Cl	373 (4.24), 402 (4.23), 480 (4.51), 5.82 (3.45), 617 (3.34)	2152 (75), 2153 (100), 2154 (87), 2155 (60), 2156 (41), 2157 (20)
Cu ^I (ChP)	417 (5.32), 540 (4.35)	2156 (80), 2157 (100), 2158 (83), 2159 (60), 2160 (39), 2161 (24)
Co ^I (ChP)	412 (5.15), 528 (4.11)	2154 (82), 2155 (100), 2156 (88), 2157 (58), 2158 (44), 2159 (27)

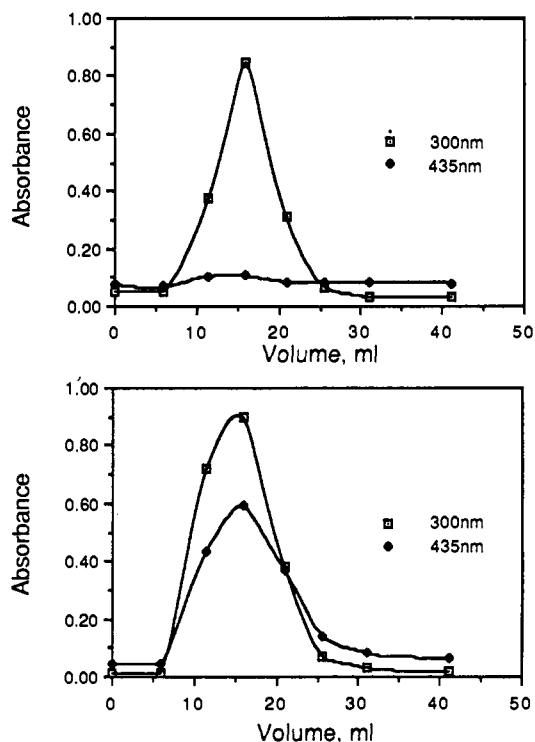


Figure 5. Gel permeation chromatography of DMPC vesicles: (top) DMPC vesicles without any porphyrin; (bottom) DMPC vesicles containing 1 mol % Cu^I(ChP).

at ambient temperature. To verify that the steroidal porphyrin was incorporated into the vesicle, a gel permeation column was run (Figure 5). The eluting fractions were monitored at 300 and 435 nm for vesicle and porphyrin, respectively. Comparison of the elution volume of a vesicle preparation without porphyrin with that of a vesicle with the steroidal porphyrin showed retention times that were the same and indicated the coelution of the porphyrin with the vesicles. Since it was also found that the steroidal porphyrin by itself did not form vesicles nor did it elute on the gel column because it is not water soluble, the coelution of the porphyrin with the bilayer vesicle clearly indicated that the porphyrin was incorporated within the bilayer.

Further proof that a normal vesicular system had indeed formed upon sonication of steroid porphyrin and DMPC was obtained using ³¹P NMR and Eu(NO₃)₃ as a shift reagent. DMPC vesicles gave ³¹P NMR spectra (Figure 6), showing a singlet at about δ -0.6 (H₃PO₄ as reference). Upon addition of the lanthanide shift reagent, the peak split into two singlets corresponding to an inner and outer phosphocholine moiety since the shift reagent can interact only with the phosphocholine group on the outer side of the vesicle.¹⁴ The same experiment with a DMPC vesicle con-

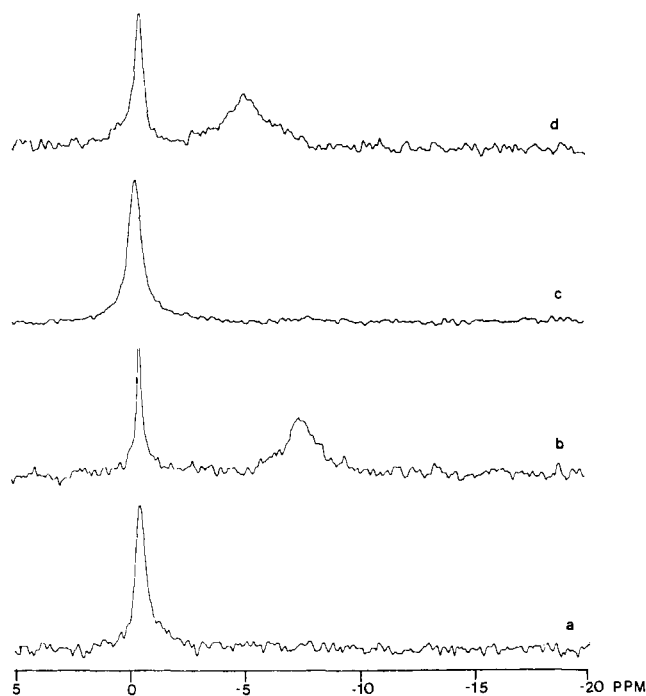


Figure 6. ^{31}P NMR of bilayer vesicles containing $\text{Cu}^{\text{II}}(\text{ChP})$: (a) 30 μmol of DMPC in 2 mL of 20% $\text{D}_2\text{O}/\text{H}_2\text{O}$; (b) 30 μmol of DMPC and 4 μmol of $\text{Eu}^{\text{III}}(\text{NO}_3)_3$ in 3 mL of 20% $\text{D}_2\text{O}/\text{H}_2\text{O}$; (c) 30 μmol of DMPC and 0.6 μmol of $\text{Cu}^{\text{II}}(\text{ChP})$ in 2 mL of 20% $\text{D}_2\text{O}/\text{H}_2\text{O}$; (d) 30 μmol of DMPC, 0.6 μmol of $\text{Cu}^{\text{II}}(\text{ChP})$, and 4 μmol of $\text{Eu}^{\text{III}}(\text{NO}_3)_3$ in 3 mL of 20% $\text{D}_2\text{O}/\text{H}_2\text{O}$.

taining $\text{Cu}^{\text{II}}(\text{ChP})$, similarly, gave two singlets, demonstrating that the steroidal porphyrin intercalated into the bilayer and that the usual spherical enclosed vesicle had formed. Further confirmation of normal vesicle formation was demonstrated by differential scanning calorimetry (DSC). It is known that the addition of cholesterol to a bilayer causes the broadening of the transition point endotherm¹⁵ (transition from gel to liquid crystalline phases). Since $\text{H}_2(\text{ChP})$ contains four cholesterol type appendages, it might also be expected to cause such a broadening in the DSC plot. Indeed, DSC plots of large multilayer DMPC vesicles containing 2.5 mol % $\text{Cu}^{\text{II}}(\text{ChP})$ showed broadening of the transition point endotherm centered around the transition temperature at 24 $^\circ\text{C}$.

Orientation of the Porphyrin Plane in the Membrane Bilayer.

The above described assays show that the steroidal porphyrin was intercalated into the bilayer vesicle and the formed vesicle has the same physical properties as synthetic DMPC vesicles without steroidal porphyrin. However, nothing about the specific configuration as indicated in Figure 1 has been demonstrated. The first objective was to determine the orientation of the heme ring in the porphyrin-bilayer assembly. In the past a myriad of techniques have been used to determine the orientation of various molecules in synthetic membrane systems. Polarized absorption spectroscopy has been used to determine the orientation of chlorophyll¹⁶ and cytochrome oxidase¹⁷ in orientated lipid bilayers. For chlorophyll in black lipid membranes (BLM), photovoltage spectroscopy has also been used.¹⁸ ESR has been useful in determining the orientation of the alkyl chains of phospholipids in bilayers by use of nitroxyl spin labels.¹⁹ Most recently the

(14) (a) Lawaczeck, R.; Kainosho, M.; Girardet, J.-L.; Chan, S. I. *Nature* **1975**, *256*, 584. (b) Ohno, H.; Maeda, Y.; Tsuchida, E. *Biochim. Biophys. Acta* **1981**, *642*, 27.

(15) Ladbroke, B. D.; Williams, R. M.; Chapman, D. *Biochim. Biophys. Acta* **1968**, *150*, 333.

(16) (a) Steineman, A.; Stark, G.; Lauger, P. J. *Membr. Biol.* **1972**, *9*, 177. (b) Cherry, R. J.; Kwan, H.; Chapman, D. *Biochim. Biophys. Acta* **1972**, *267*, 512.

(17) Blasie, J. K.; Erecinska, M.; Samuels, S.; Leigh, J. S. *Biochim. Biophys. Acta* **1978**, *501*, 33.

(18) Weller, H. G.; Tien, H. T. *Biochim. Biophys. Acta* **1973**, *325*, 433.

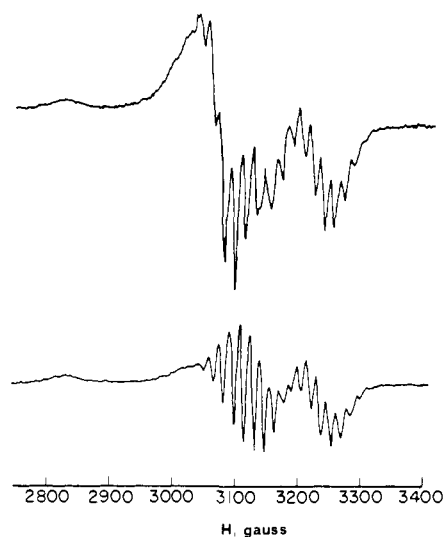


Figure 7. Isotropic ESR spectra of $\text{Cu}^{\text{II}}(\text{ChP})$ in chloroform and vesicular solution. (top) Spectrum of vesicular solution of 10 μmol of DMPC and 0.5 μmol of $\text{Cu}^{\text{II}}(\text{ChP})$ in 1 mL of H_2O : Microwave power 10 mW, microwave frequency 9055 MHz, modulation frequency 100 KHz, modulation amplitude 5 G, time constant 0.3 s, scan time 4 min, temperature 77 K, receiver gain 2×10^3 . (bottom) Spectrum of 1.3 mmol of $\text{Cu}^{\text{II}}(\text{ChP})$ in chloroform: Microwave power 2 mW, microwave frequency 9053 MHz, modulation frequency 100 KHz, modulation amplitude 1 G, time constant 1.0 s, scan time 8 min, temperature 77 K, receiver gain 2×10^3 .

orientations of a copper phthalocyanine²⁰ and a copper tetrapyrrolineporphyrine²¹ in Langmuir-Blodgett films have been determined by use of ESR spectra of the paramagnetic copper species.

We have determined the orientation of the porphyrin ring in the bilayer assembly to be parallel to the aqueous-bilayer interface by using the ESR spectrum of $\text{Cu}^{\text{II}}(\text{ChP})$ as a molecular probe. ESR spectra of $\text{Cu}^{\text{II}}(\text{ChP})$ were taken both in chloroform and vesicular solution (Figure 7). These two similar spectra are very characteristic of isotropic copper(II) porphyrin spectra.²² This indicates that the $\text{Cu}^{\text{II}}(\text{ChP})$ does not self-orient in homogeneous chloroform solution and that intercalation alone in the bilayer does not alter the ESR spectrum. Preparation of an *oriented bilayer assembly* containing $\text{Cu}^{\text{II}}(\text{ChP})$, where bilayers are stacked on an inert surface, have afforded anisotropic ESR spectra and have allowed the determination of the orientation of the porphyrin ring in the bilayer. Thus, we have prepared an oriented bilayer assembly containing 1 mol % $\text{Cu}^{\text{II}}(\text{ChP})$ on a sheet of Mylar polymer according to methods described in the literature.²³ DMPC vesicles containing 1 mol % $\text{Cu}(\text{ChP})$ were prepared by sonicating a thin film in distilled water for 30 s. The resultant milky dispersion was spread on a Mylar sheet, and the excess water was evaporated on standing at room temperature for 6 h. The edges of the formed oriented bilayer film were then carefully scraped away, and the film was cut into 3-mm strips. A total of 15 of these strips were then bundled together and placed in an ESR tube, and spectra were taken at various angles of the film relative to the magnetic field.

Figure 8 shows the anisotropic ESR spectra of the oriented bilayer at various angles where θ is the angle between the magnetic field and the normal to the plane of the Mylar strips. As expected, the differences between the isotropic and anisotropic spectra are

(19) Hubbell, W. L.; McConnell, H. M. *Proc. Natl. Acad. Sci.* **1969**, *64*, 20.

(20) Cook, M. J.; Daniel, M. F.; Dunn, A. J.; Gold, A. A.; Thomsom, A. J. *J. Chem. Soc., Chem. Commun.* **1986**, 863.

(21) Palacin, S.; Ruaudel-Teixier, A.; Beraud, A. *J. Phys. Chem.* **1986**, *90*, 6237.

(22) Monoharan, P. T.; Rogers, M. T. In *Electron Spin Resonance of Metal Complexes*; Yen, T. F., Ed.; Plenum: New York, 1969; p 143.

(23) (a) Libertini, L. J.; Waggoner, A. S.; Jost, P. C.; Griffith, O. H. *Proc. Natl. Acad. Sci.* **1969**, *64*, 13. (b) Bangham, A. D.; Horne, R. W. *J. Mol. Biol.* **1964**, *8*, 660.

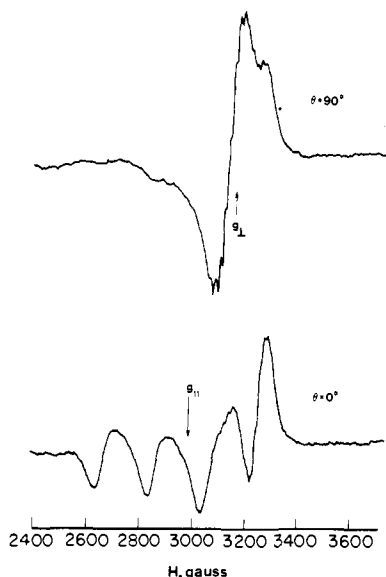


Figure 8. ESR spectra of $\text{Cu}^{\text{II}}(\text{ChP})$ in an orientated bilayer assembly. (top) Magnetic field is parallel to the Mylar film, $\theta = 90^\circ$. (bottom) Magnetic field is perpendicular to the Mylar film, $\theta = 0^\circ$. Spectral conditions: microwave power 1 mW, microwave frequency 9055 MHz, modulation frequency 100 KHz, modulation amplitude 5 G, time constant 1.0 s, scan time 8 min, temperature 77 K, receiver gain 3.2×10^3 . The angle θ is defined as the angle between the magnetic field and the normal to the plane of the Mylar strips.

very distinct. For $\theta = 0^\circ$ the signal is composed of four equidistant peaks at $g_{\parallel} = 2.162$, and for $\theta = 90^\circ$ the signal is composed of a single line at $g_{\perp} = 2.047$. At angles between these two extremes the signal is a hybrid of the spectra described above, the relative intensities being a function of the angle. Published ESR spectra of copper tetraphenylporphyrin (CuTPP) single crystals²² show that when the applied static magnetic field is parallel ($\theta = 0^\circ$) to the 4-fold molecular axis of the heme, one obtains a spectrum of four sets of lines due to the interaction of the unpaired electron with the copper nuclei ($I = 3/2$). The g value found was $g_{\parallel} = 2.190$. In addition superhyperfine lines due to interaction of the unpaired electron with the four nitrogens of the pyrrole groups were observed. When the magnetic field is perpendicular ($\theta = 90^\circ$) to the molecular axis, the lines merge together to form a single line at $g_{\perp} = 2.045$. Therefore, comparison of the spectra of CuTPP single crystals and the copper steroidal porphyrin in the orientated bilayer clearly enables one to deduce that the porphyrin plane of $\text{Cu}^{\text{II}}(\text{ChP})$ was perpendicular to the bilayer normal (parallel to the Mylar film). Loss of the majority of the superhyperfine structure of the spectra is probably due to coupling interactions because of stacking of the bilayer in the sample.

Determination of the Position of the Porphyrin Plane in the Membrane Bilayer. A necessary prerequisite for the steroidal-bilayer assembly to be a site-selective catalytic system is for the plane of the porphyrin to be at a fixed and predictable distance from the water-lipid interface. If the plane of the porphyrin ring is in a known defined position, then substrates that also have specific alignments in bilayers such as sterols and fatty acids with more than one reactive position may be selectively modified by epoxidation. Ideally, the steroidal porphyrin will span a DMPC bilayer with the porphyrin centered between the two phospholipid layers. However, bilayers are not rigid entities and considerable molecular motion may be expected. Therefore, although on the average the porphyrin ring may be in the bilayer center, large structural fluctuations may give rise to a disordered system having poor regioselective qualities. Using the ligation of specifically constructed imidazolyl ligands to $\text{Co}^{\text{II}}(\text{ChP})$ as a molecular probe, we have determined that not only is the porphyrin plane centered in a DMPC bilayer but fluctuations of the heme ring from the center are relatively small, on the order of 3–4 Å.

It has been known for several years that the ESR spectra of cobalt(II) porphyrins are very sensitive to axial ligation²⁴ because

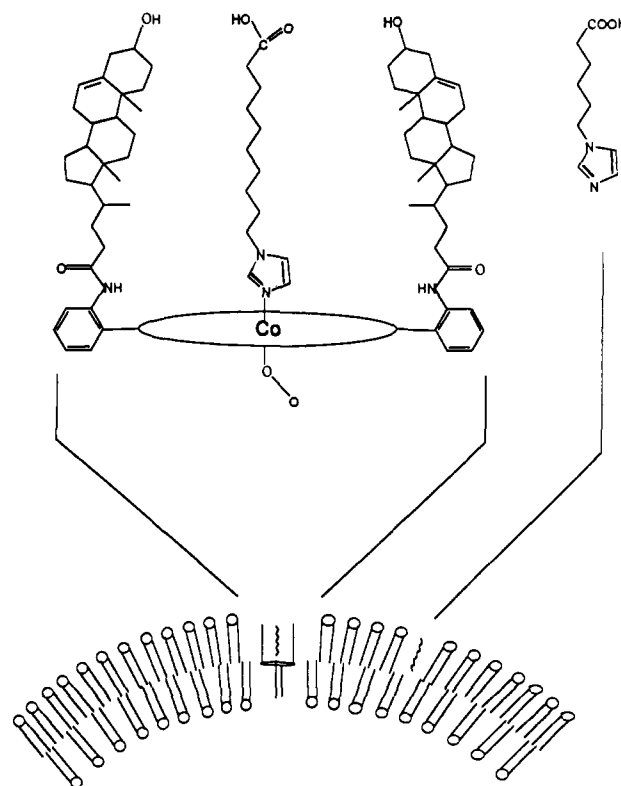


Figure 9. Idealized drawing of the interaction of tethered imidazole ligands and $\text{Co}^{\text{II}}(\text{ChP})$ in a bilayer.

of the single unpaired electron in the d_{z^2} orbital. Thus, examination of cobalt(II) porphyrin ESR spectra has enabled the differentiation between four-, five-, and six-coordinate species. We took advantage of this property and synthesized imidazole ligands tethered with carboxylic acids (see the Experimental Section). These molecules have an imidazole ligand at one end and a carboxylic acid at the other, with an alkyl chain of varied length separating the two groups [$\text{Im}(\text{CH}_2)_n\text{COOH}$]. These ligands when added to a vesicle solution after their formation should align themselves in a bilayer so that the carboxylic acid group is at the water-lipid interface and the alkyl chain along with the imidazole group dangles into the hydrophobic lipid phase as in Figure 9. Tethered ligands with sufficiently long alkyl chains should reach the porphyrin metal center, ligate, and then cause a change in the ESR spectrum. In this manner the variation of the alkyl chain could enable measurement of the position of the porphyrin plane in the bilayer.

Figure 10 shows the ESR spectra of $\text{Co}^{\text{II}}(\text{ChP})$ in both a homogeneous chloroform solution and DMPC vesicles.²⁵ The two spectra are very similar with the major feature at a field of 2800 G, $g = 2.35$ (the peak at 2400 G is from an impurity in the cavity). These spectra are typical of five-coordinate cobalt(II) porphyrins with solvent molecules as weak axial ligands.²⁴ Upon addition of the tethered imidazole ligands, two different spectra were observed depending on the length of the alkyl chain (Figure 11). For ligands where $n = 2, 4, 5$ the resulting spectra were unchanged from the spectrum of $\text{Co}^{\text{II}}(\text{ChP})$ in vesicles without added ligand. For ligands where $n = 7, 9$ a new ESR spectrum was found with the major feature at 3200 G, $g = 2.0$. This spectrum is typical of a six-coordinate cobalt(III)-superoxide complex with a nitrogen base as the sixth axial ligand.^{24,25b} Clearly there is a dependence

(24) (a) Walker, F. A. *J. Am. Chem. Soc.* **1970**, *92*, 4235. (b) Walker, F. A. *J. Magn. Reson.* **1974**, *15*, 201.

(25) (a) Spectra were taken in a nitrogen atmosphere to prevent auto-oxidation of $\text{Co}^{\text{II}}(\text{ChP})$. (b) It is tempting to speculate that the imidazoles are preferentially ligated to cobalt from the *outside* of the spherical vesicles and, accordingly, O_2 is coordinated on the *inside* face. We are currently examining this approach to metalloporphyrin-mediated vectorial processes across synthetic bilayers.

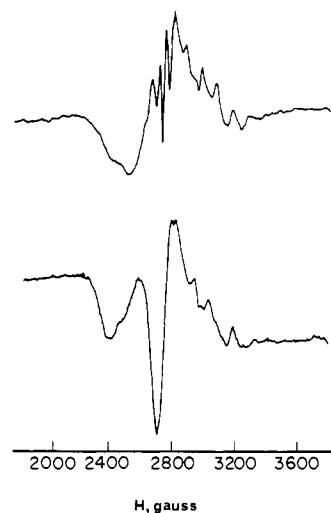


Figure 10. ESR spectra of $\text{Co}^{\text{II}}(\text{ChP})$ in chloroform and DMPC vesicles. (top) 0.5 mmol of $\text{Co}^{\text{II}}(\text{ChP})$ in CHCl_3 : microwave power 20 mW, microwave frequency 9040 MHz, modulation frequency 100 KHz, modulation amplitude 20 G, time constant 1.0 s, scan time 8 min, temperature 77 K, receiver gain 3.2×10^3 . (bottom) Spectrum of a vesicular solution containing 3 μmol of DMPC and 0.03 μmol of $\text{Co}^{\text{II}}(\text{ChP})$, in 0.3 mL of H_2O : microwave power 20 mW, microwave frequency 9028 MHz, modulation frequency 100 KHz, modulation amplitude 20 G, time constant 1.0 s, scan time 8 min, temperature 77 K, receiver gain 4×10^3 .

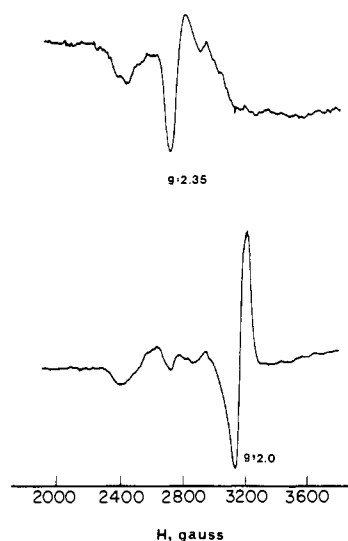


Figure 11. ESR spectra of $\text{Co}^{\text{II}}(\text{ChP})$ in vesicular solution with added tethered imidazole ligands. (top) Spectrum of a vesicular solution containing 3 μmol of DMPC, 0.03 μmol of $\text{Co}^{\text{II}}(\text{ChP})$, and 0.6 μmol of 6-imidazolylhexanoic acid in 0.3 mL of H_2O : microwave power 20 mW, microwave frequency 9028 MHz, modulation frequency 100 KHz, modulation amplitude 20 G, time constant 1.0 s, scan time 8 min, temperature 77 K, receiver gain 4×10^3 . (bottom) Spectrum of a vesicular solution containing 3 μmol of DMPC, 0.03 μmol of $\text{Co}^{\text{II}}(\text{ChP})$, and 0.6 μmol of 8-imidazolyl octanoic acid in 0.3 mL of H_2O : microwave power 20 mW, microwave frequency 9028 MHz, modulation frequency 100 KHz, modulation amplitude 20 G, time constant 1.0 s, scan time 8 min, temperature 77 K, receiver gain 1.25×10^3 .

on the length of the alkyl chain separating the carboxylic acid and imidazole groups of the tethered ligand. For $n < 6$ there is no ligation and therefore no change in the ESR spectrum; the imidazole group did not reach the metal center. For $n > 6$ there is ligation; a change in the ESR spectrum was observed, indicating that the imidazole did reach the metal center. From molecular models one may approximate the distance from the carboxylic acid group to the binding nitrogen of the imidazole ring to be about 15–16 Å for $n = 6$. Since the width of a DMPC bilayer has been measured at 35–40 Å,²⁶ one finds that tethered ligands within 3–4

Table II. Epoxidation of Sterols

substrate	product	bilayer assembly: ^a yield, ^c %	homogeneous solution ^b for FeTpTPCl (FeChPcl)	
			yield, ^d %	relative reactivity $\Delta^5/\text{side chain}^{\text{e,f}}$
cholesterol	5,6-epoxide	0	31.2 (10.1)	
desmosterol	5,6-epoxide	0 (0) ^g	26.8 (6.8)	3.6 (4.0)
	24,25-epoxide	32.0 (27.1) ^g	7.3 (1.7)	
fucosterol	5,6-epoxide	0	26.4	3.2
	24,28-epoxide	22.2	8.3	3.2
stigmaterol	5,6-epoxide	0	28.7 (7.5)	18 (15)
	22,23-epoxide	trace	1.6 (0.5)	

^a Reaction conditions: 1.0 μmol of sterol, 0.1 μmol of $\text{Fe}^{\text{III}}(\text{ChP})\text{Cl}$, 10 μmol of DMPC, 1 μmol of PhIO as 20 mM solution 1/1 methanol/water in 4 mL of phosphate buffer (pH 7.4), 30 °C, time 2 h.

^b Reaction conditions: 2.0 μmol of sterol, 0.2 μmol of FeTpTPCl or $\text{Fe}(\text{ChP})\text{Cl}$ results in parentheses, 70 μL of CH_2Cl_2 , 4.0 μmol of PhIO as a solid, room temperature, time 2 h. ^c Yields based on starting sterols. ^d Yields in parentheses for $\text{Fe}^{\text{III}}(\text{ChP})\text{Cl}$ as catalyst. ^e Ring epoxidation gave a 3/1 ratio of $5\beta,6\beta/5\alpha,6\alpha$ -epoxide. ^f Values in parentheses for $\text{Fe}^{\text{III}}(\text{ChP})\text{Cl}$ as catalyst. ^g Reaction done with DPPC in place of DMPC.

Å of the bilayer center will bind to the $\text{Co}^{\text{II}}(\text{ChP})$ whereas those further away will not do so. This *plumb bob* experiment clearly places the heme ring of the steroidal porphyrin in the bilayer center with minor fluctuation around that center.

Site-Selective Oxidations. Above we have shown that this pillared steroidal metalloporphyrin bilayer assembly is a highly ordered system with the porphyrin ring centered in the bilayer and parallel to the bilayer plane. This specific configuration has enabled the selective oxidation of substrates that are amphiphilic and bilayer compatible using either $\text{Fe}^{\text{III}}(\text{ChP})\text{Cl}$ or $\text{Mn}^{\text{III}}(\text{ChP})\text{Cl}$ as catalysts. Sterols and fatty acids were found to be particularly suitable membrane compatible substrates. Therefore, we have examined the epoxidation of sterols with alkene moieties both at the B ring (the Δ^5 bond) and the side chain, the epoxidation of polyunsaturated fatty acids and isomers of octadecenoic acid, and the hydroxylation of cholesterol. In addition, we have investigated the hydroxylation of lipophilic alkanes in a bilayer environment.

A typical reaction in a vesicle entailed the following protocol. DMPC vesicles were prepared by ultrasonication of a thin film of 10 μmol of DMPC, 1–2 of μmol substrate, and 0.05–0.1 μmol of metalated steroidal porphyrin in the presence of phosphate buffer, pH 7.4. After equilibration of the vesicular solution, the primary oxidant, e.g., iodosylbenzene or sodium periodate, was introduced to the aqueous phase. After completion of the reaction, ether was added and the vesicles were destroyed by vigorous agitation. Fatty acids were methylated with diazomethane, and the reaction mixture was purified over a dry alumina column prior to analysis by GC and GC/MS. The steroid epoxidations (Table II) showed that the $\text{Fe}(\text{ChP})\text{Cl}$ -bilayer assembly was a site-selective catalytic system. All sterols were epoxidized exclusively on the side chain,²⁷ whereas epoxidations in homogeneous systems with $\text{Fe}^{\text{III}}(\text{ChP})\text{Cl}$ or (*meso*-tetra-*p*-tolylporphyrin)iron(III) chloride [$\text{Fe}(\text{TpTP})\text{Cl}$] showed the Δ^5 double bond to be considerably more reactive than that on the side chain. It is clear that the intercalation of the catalyst into the bilayer enables highly regioselective epoxidation on the side chain. This high selectivity was further demonstrated by the fact that stigmaterol with a Δ^{22} double bond only two bond lengths further removed from the hydrophobic end was unreactive. Yields and catalyst turnovers were found to be amplified by addition of oxidant in small portions. For example, a yield of 68% (27.2 turnovers) of 24,25-epoxy-

(26) (a) Elbers, P. F.; Ververgaert, J. T. *J. Cell Biol.* **1965**, *25*, 375. (b) Chapman, D.; Williams, R. M.; Ladbrooke, B. D. *Chem. Phys. Lipids* **1967**, *1*, 445. (c) Engelman, D. M. *J. Mol. Biol.* **1970**, *47*, 115.

(27) Selective side-chain epoxidation has been achieved by an intramolecular template effect. See ref 9 and Breslow, R.; Maresca, L. M. *Tetrahedron Lett.* **1977**, 623.

Table III. Epoxidation of Polyunsaturated Fatty Acids

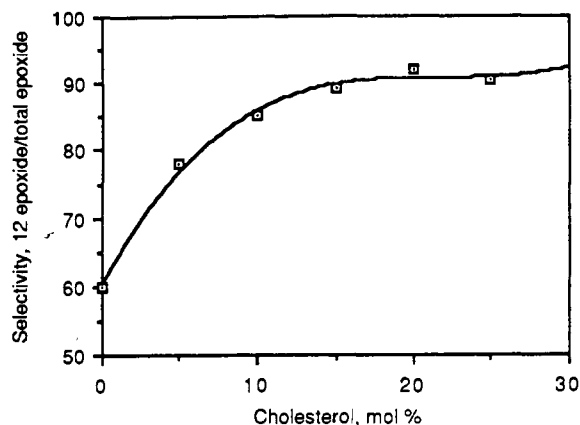
substrate	bilayer assembly of Fe ^{III} (ChP)Cl ^a		homogeneous solution of FeTpTPCl/CH ₂ Cl ₂ ^b	
	yield, ^a %	ratio epoxides ^d	yield, ^c %	ratio epoxides ^d
linoleic acid	32.0	1.7	7.5	1.0
linoleic acid ^e	28.0	1.9		
linoleic acid ^f	23.0	2.0		
linoleic acid ^g	27.0	1.8		
9,12(<i>E,E</i>)- octadecadienoic acid	8.0	1.4	2.5	1.0
11,14(<i>Z,Z</i>)- eicosadienoic acid	16.0	1.3	8.1	1.0
methyl linoleate	25.0	1.5	9.0	1.0

^a Reaction conditions: 1.0 μmol of substrate, 0.1 μmol of Fe^{III}(ChP)Cl, 10 μmol of DMPC, 1.0 μmol of iodobenzene as a 20 mM solution in 1/1 methanol/water in 4 mL of phosphate buffer (pH 7.4), 30 °C, time 2 h. ^b Reaction conditions: 2.0 μmol of substrate, 0.2 μmol of Fe^{III}(ChP)Cl, 70 μL of CH₂Cl₂, 2.0 μmol of iodobenzene as a solid, room temperature, time 2 h. ^c Yields based on starting fatty acid. ^d Ratio of diprophobic/hydrophilic end monoepoxides. ^e Reaction done with dipalmitoylphosphocholine. ^f Temperature 5 °C. ^g Temperature 50 °C.

desmosterol could be obtained in a vesicular solution containing 10 μmol of DMPC, 2.0 μmol of desmosterol, and 0.05 μmol of Fe^{III}(ChP)Cl by six periodic additions of 2.0-μmol aliquots of iodobenzene. Fucosterol was found to be slightly less reactive than desmosterol possibly because the alkene moiety is more hindered.

The epoxidation of polyunsaturated fatty acids (Table III) was considerably less regioselective. The epoxidation of the double bond closer to the hydrophobic terminus in the bilayer was favored by less than 2:1. The length of the fatty acid chain was only of minor consequence, C₂₀ fatty acids being epoxidized with only slightly less selectivity versus C₁₈ fatty acids. Esterification of the carboxylic acid had little effect, and trans isomers gave lower yields as expected.²⁸ The site selectivity was relatively temperature insensitive although yields varied slightly. The reduced site selectivity for fatty acid epoxidation may be due to the fact that the rigidity of phospholipid bilayers is known to decrease significantly upon the addition of unsaturated fatty acids into the bilayer.²⁹ These acids in the bilayer cause a dramatic decrease in the gel to liquid crystalline phase-transition temperature, the latter being a measure of membrane rigidity. For example, the transition temperature of the partially unsaturated egg yolk bilayer is -15 °C, whereas for DMPC it is 24 °C. The loss of rigidity is due to the formation of kinks, and this in turn enables fluctuations in the bilayer width and leads directly to reduced regioselective epoxidation.

From the above results of fatty acid epoxidation it would appear at first glance that epoxidations of substrates, which considerably reduce the rigidity of the bilayer assembly, would severely limit the usefulness of the catalytic system for regioselective epoxidation. However, we have found that this reduction of rigidity can be controlled and reversed by the addition of cholesterol to the bilayer. Cholesterol is unreactive toward epoxidation with the vesicular catalyst (Table II), and it is known to cause an increase in bilayer rigidity.³⁰ The addition of cholesterol to Fe(ChP)-bilayer assemblies gave rise to a very significant increase in the regioselectivity of epoxidation at the Δ¹² position of linoleic acid (9,12-(*Z,Z*)-octadecadienoic acid; Figure 12). Interestingly, this increase in selectivity leveled off after the addition of about 20 mol % of cholesterol to the DMPC bilayer. This is in agreement with past findings that in vesicles with more than 20 mol % cholesterol

**Figure 12.** Selectivity of linoleic acid epoxidation in vesicular solution as a function of the cholesterol content of the bilayer.**Table IV.** Epoxidation of Isomeric Octadecenoic Acids

substrate	yield, ^a %	substrate	yield, ^a %
6(<i>Z</i>)-octadecenoic acid (petroselinic)	2.3	11(<i>Z</i>)-octadecenoic acid (vaccenic)	25.5
9(<i>Z</i>)-octadecenoic acid (oleic)	6.8		

^a Yield based on starting fatty acid. ^b Reaction conditions: 1.0 μmol of octadecenoic acid, 0.1 μmol of Mn^{III}(ChP)Cl, 10 μmol of DMPC, 1.0 μmol of sodium periodate in 2 mL of phosphate buffer (pH 7.4), time 2 h.

Table V. Hydroxylation of Saturated Hydrocarbons and Cholesterol^a

substrate	method	yield, % mol product/mol	
		substrate	product
cyclooctane	I	8.5	cyclooctanone
cyclooctane	II	15.5	cycloctanol/cyclooctanone (12/1)
adamantane	I	4.0	admantan-1-ol
ethylbenzene	I	15.0	acetophenone
ethylbenzene	II	22.0	1-hydroxyethylbenzene/acetophenone (8/1)
fluorene	I	5.8	9-fluorenone
cholesterol	I	2.0	25-hydroxycholesterol

^a Reaction conditions. Method I: Vesicles containing 10 μmol of DMPC, 2.0 μmol of substrate, and 0.05 μmol of Mn^{III}(ChP)Cl were formed in 2 mL of a Tris pH 8.6 buffer. The solution was purged with oxygen, and 100 μmol of ascorbic acid was added. The reaction time was 15 h. Method II: Vesicles containing 10 μmol of DMPC, 2.0 μmol of substrate, 0.25 μmol of *N*-1-pentylimidazole, and 0.05 μmol of Mn^{III}(ChP)Cl were formed in 2 mL of phosphate pH 7.4 buffer. 10 μmol of sodium periodate were added as oxidant after 15 min. Reaction time was 3 h.

two domains are formed, one rich in cholesterol and one lacking the sterol.³¹ Epoxidation in the cholesterol-poor domain would be expected to remain less site selective, reducing the net regioselectivity of the reaction.

From the results of the linoleic acid epoxidation, one can discern higher yields in the bilayer assembly vis-a-vis the homogeneous system at comparable concentrations. We believe this to be due to a favorable orientation effect unique to the bilayer system since diffusion of the fatty acid within the bilayer is limited to two dimensions. This limitation in the degrees of freedom would increase the likelihood of productive collisions leading to reaction. This phenomenon would also explain the increased yields in the sterol epoxidation when Fe^{III}(ChP)Cl is in the bilayer versus the homogeneous system. It has been recognized in the past that the stability of the metalloporphyrin in the presence of oxidant is concentration dependent.³² Therefore, higher effective reactivity

(28) Groves, J. T.; Nemo, T. E. *J. Am. Chem. Soc.* **1983**, *105*, 5786.
 (29) Ladbrooke, B. D.; Chapman, D. *Chem. Phys. Lipids* **1969**, *3*, 304.
 (30) (a) Papahadjopoulos, D.; Kimelberg, H. K. *Prog. Surf. Sci.* **1973**, *4*, 180. (b) Hsia, J. C.; Scheider, H.; Smith, I. C. P. *Chem. Phys. Lipids* **1970**, *4*, 238. (c) Lee, A. G.; Birdsall, N. S. M.; Levine, V. K.; Metcalfe, J. C. *Biochim. Biophys. Acta* **1972**, *255*, 43. (d) Darke, A.; Finer, E. G.; Flook, A. G.; Phillips, M. C. *J. Mol. Biol.* **1972**, *63*, 265.

(31) Darke, A.; Finer, E. G.; Flook, A. G.; Phillips, M. C. *FEBS Lett.* **1971**, *18*, 326.

in the bilayer would increase the stability of the catalyst and increase yields.

Another manifestation of the regioselectivity of the bilayer assembly can be seen in the epoxidation of isomeric octadecenoic acids (Table IV). In this case the site selectivity resulted in positional variations in epoxide yields. As may be expected, the closer the alkene moiety to the hydrophobic terminus, the higher the yield. Thus the reactivity decreased in the order $\Delta^{11} > \Delta^9 > \Delta^6$.

The utility of the bilayer assembly was not limited to epoxidation reactions. We have found that a $Mn^{III}(ChP)Cl$ system was able to hydroxylate alkanes and to selectively hydroxylate cholesterol at the C_{25} position³³ (Table V). Hydroxylations in vesicular solutions were carried out either under aerobic conditions with sodium ascorbate as the reducing agent³⁴ (method I) or with sodium periodate as primary oxidant³⁵ (method II). The former oxidizing system has the advantage of not causing significant catalyst decomposition; however, the reaction is very slow. The later system is much more reactive; however, fast catalyst decomposition occurred in the presence of the less reactive alkanes. Therefore, although the yields were low in all cases, the vesicular assembly can still be considered a viable hydroxylation system. The aerobic system oxidized secondary alcohols to ketones. Most importantly, cholesterol was selectively hydroxylated to give exclusively 25-hydroxycholesterol leaving the more chemically reactive Δ^5 double bond untouched due to its inaccessibility. This selective C_{25} hydroxylation was more efficient on a per hydrogen basis than the hydroxylation of adamantane. We attribute this effect to the proximity of the C_{25} tertiary carbon to the metal center. The identity of the product was confirmed by GC and GC-MS (see Experimental Section).

Another point of interest concerning an oxidation reaction in bilayer assemblies concerns the fate of the product after it is formed. There are two possible scenarios. The first is that the product is sufficiently hydrophilic or bilayer incompatible so that it diffuses out of the vesicle into the aqueous phase or to bilayer interface. The second possibility is that the product is sufficiently hydrophobic or membrane compatible to remain in the membrane. The hypothesis was not tested for hydroxylations because of the low reaction yields; however, results of epoxidations in two different systems show that the later pathway is dominant for epoxide products. In an internal olefinic system as exemplified by linoleic acid epoxidation under conditions described in Table III, we have found that, in addition to the monoepoxide yield of about 30%, two isomeric diepoxides were formed in a 2–3% yield. Considering the reduced reactivity of the Δ^9 position, this result indicates that the monoepoxide did not diffuse out of the hydrophobic bilayer phase. In order to test the hypotheses for terminal olefins, *p*-divinylbenzene was chosen as a substrate. Models with this substrate show that if the monoepoxide should diffuse out of the vesicle after its formation, the second double bond would no longer be accessible to the reactive site for geometric reasons. Vesicles were prepared containing 10 μ mol of DMPC, 2 μ mol of *p*-divinylbenzene, and 0.1 μ mol of $Mn^{III}(ChP)Cl$ in 2.0 mL of phosphate buffer, pH 7.4, and 1.2 μ mol of iodosylbenzene was added. Analysis after 2 h showed a 27.2% monoepoxide yield and a 4.1% diepoxide yield. The results clearly indicate that the monoepoxides of terminal and internal diolefins are sufficiently hydrophobic and bilayer compatible to remain in the bilayer phase and undergo epoxidation at the second available site.

Conclusion

A membrane-compatible porphyrin has been synthesized by appending cholenic acid moieties to a tetrakis(aminophenyl)-

porphyrin. This steroidal porphyrin has been shown to span a vesicle bilayer in such a manner that the porphyrin ring is centered in the bilayer center with only ± 3 –4-Å fluctuations and lies parallel to the aqueous interface. The iron(III) and manganese(III) metalloporphyrins in bilayer assemblies have been shown to be active and site-selective catalysts for the epoxidation and hydroxylation of membrane-compatible substrates such as sterols and fatty acids.

Experimental Section

Instruments and Materials. Compounds accessible from commercial sources were of the highest purity available and used without further purification with the exception of THF, which was distilled over K-Na. The following instruments were used: 1H NMR, General Electric QE-300; ^{31}P NMR, Bruker WM-250; DSC, Perkin-Elmer DSC-4; GC, Hewlett Packard 5890; FABMS and GC-MS, Kratos MS50; EPR, Varian E-12; UV-vis, Cary 2130 and IBM 9430.

Preparation of the Steroidal Porphyrin $H_2(ChP)$. In a 100-mL round-bottomed flask, 3 g of 3β -hydroxy-5-cholenic acid (Sigma) and 50 mL of 85% formic acid were stirred as a suspension at 90–95 °C for 3 h (a slight greenish color was observed). The suspension was cooled and 100 mL of water added. The solution was filtered on the pump, yielding 2.95 g of crude 3β -formato-5-cholenic acid. The crude product was dissolved in methylene chloride and treated with activated carbon, and the methylene chloride was evaporated off, yielding 2.8 g (87% yield) of slightly yellowish solid, mp 160–163 °C. 1H NMR ($CDCl_3$, 300 MHz): δ 8.06 (1 H, s, formate), 4.75 (1 H, br s, C_6), 1.05 (3 H, s, C_{19}), 0.96 (3 H, d, C_{21}), 0.71 (3 H, s, C_{18}), 2.4–0.6 (26 H, m).

meso-Tetrakis(*o*-aminophenyl)porphyrin, H_2TamPP , was prepared according to the literature procedure.³⁶ The $\alpha,\beta,\alpha,\beta$ atropisomer was separated as the fastest moving fraction by column chromatography on a 40 cm by 5 cm silica gel column (Merck Kieselgel, 70–230 mesh) with 15% ethyl acetate–85% chloroform as eluent, R_f 0.75–0.80.

In a 100-mL round-bottomed flask were dissolved 67.5 mg (0.1 mmol) of well-dried $\alpha,\beta,\alpha,\beta$ - H_2TamPP and 12.2 mg (0.1 mmol) of well-dried 4-(dimethylamino)pyridine in 20 mL of dry THF (distilled over K-Na). In a separate flask 402 mg (1 mmol) of dried 3β -formato-5-cholenic acid and 101 mg (1 mmol) of triethylamine (Aldrich Gold Label stored over KOH) were added to 15 mL of dry THF and cooled in an ice bath. A total of 1 mmol of isobutyl chloroformate was slowly added by syringe and the mixture stirred for 10 min. The resulting mixed anhydride was then added as is to the $\alpha,\beta,\alpha,\beta$ - H_2TamPP solution. After 1 and 2 h additional 0.5-mmol aliquots of similarly prepared anhydride were added to the porphyrin solution. The reaction could be followed by TLC after hydrolysis of the formate ester (see below). After 4 h the reaction was stopped. A total of 250 mL of methylene chloride was added and the formate ester hydrolyzed with 50 mL of 10% NaOH in methanol by stirring for 3 min at room temperature. Water was then added, and phases were separated. The organic phase was washed twice with water and once with brine and dried over Na_2SO_4 . TLC on silica gel with 3% MeOH, 23% EtOAc, and 74% $CHCl_3$ as eluent showed two major products at $R_f = 0.22$ and $R_f = 0.08$, the desired $H_2(ChP)$ being of the greater polarity. The product was separated on a 45 cm by 5 cm silica gel column (Merck Kieselgel, 200–400 mesh). After evaporation and vacuum evacuation 82 mg of pure (TLC one spot) $H_2(ChP)$ was obtained (39% yield). $H_2(ChP)$ was light and oxygen sensitive and should be stored under nitrogen in the dark at –20 °C. 1H NMR ($CDCl_3$, 300 MHz): δ 8.88 (8 H, s, pyrrole), 8.74 (4 H, d, phenyl), 8.00 (4 H, d, phenyl), 7.89 (4 H, t, phenyl), 7.53 (4 H, t, phenyl), 6.70 (4 H, s, amide), 5.29 (4 H, d, C_6 steroid), 3.50 (4 H, br s, C_3 steroid), 0.93 (12 H, s, C_{19} steroid), 0.85 (12 H, d, C_{18} steroid), 0.31 (12 H, s, C_{21} steroid), 2.25–0.16 (104 H, m, steroid), –2.64 (2 H, s, NH pyrrole) (Figure 3). Vis (CH_2Cl_2 ; gave λ_{max} (log ϵ): 422 (5.40), 516 (4.09), 549 (3.54), 590 (3.60), 645 nm (3.30). FABMS (*m*-nitrobenzyl alcohol matrix): m/z 2099 (78), 2100 (100), 2101 (86), 2102 (59), 2103 (32), 2104 (17).

Preparation of Metalated Steroidal Porphyrins, $M(ChP)$. $Fe^{III}(ChP)Cl$. In a 25-mL round-bottomed flask, 41.5 mg (0.02 mmol) of $H_2(ChP)$, 60 mg (0.3 mmol) of anhydrous $FeBr_2$ (Alfa), and 20 mg (0.25 mmol) of pyridine (distilled over KOH) were added to 10 mL of dry THF and refluxed under argon in the drybox. After 2.5 h, the reaction was complete as monitored by the visible spectrum and the flask was opened to air for 30 min. The solvent was evaporated to a minimum and the $Fe^{III}(ChP)Br$ was purified over a 15 cm by 1 cm silica column (Merck Kieselgel, 200–400 mesh) with 3% MeOH, 23% EtOAc, and 74% $CHCl_3$ as eluent. The collected iron porphyrin was washed twice

(32) Groves, J. T.; Krishnan, S.; Avaria, G. E.; Nemo, T. E. In *Biomimetic Chemistry*; Dolphin, D., McKenna, C., Murahami, Y., Tabushi, I., Eds.; Advances in Chemistry Series No. 191; American Chemical Society: Washington, DC, 1980; p 277.

(33) Groves, J. T.; Neumann, R. *J. Org. Chem.* **1988**, *53*, 3891.

(34) Mansuy, P.; Fontecave, M.; Bartoli, J.-F. *J. Chem. Soc., Chem. Commun.* **1983**, 253.

(35) (a) Takata, T.; Ando, W. *Tetrahedron Lett.* **1983**, *24*, 3631. (b) Groves, J. T.; McMurry, T. J., unpublished results.

(36) Collman, J. P.; Gagne, R. R.; Reed, C. A.; Halbert, T. R.; Lang, G.; Robinson, W. J. *J. Am. Chem. Soc.* **1975**, *97*, 1427.

with dilute HCl and dried with Na_2SO_4 , and the solvent was evaporated, yielding 28.5 mg (65% yield) of $\text{Fe}^{\text{III}}(\text{ChP})\text{Cl}$. Vis (λ_{max} (log ϵ)): 420 (4.83), 510 (3.94), 584 (3.68), 654 nm (3.20). FABMS (*m*-nitrobenzyl alcohol matrix; $\text{M}^+ - \text{Cl}$): *m/z* 2154 (85), 2155 (100), 2156 (89), 2157 (58), 2158 (40), 2159 (25).

$\text{Mn}^{\text{III}}(\text{ChP})\text{Cl}$. In a 25-mL round-bottomed flask, 31.0 mg (0.015 mmol) of $\text{H}_2(\text{ChP})$, 500 mg (2 mmol) of manganese(II) diacetate tetrahydrate, and 16 mg (0.2 mmol) of pyridine were added to 10 mL of THF. The solution was refluxed and the reaction monitored by the visible spectrum. After 12 h the reaction was complete. CH_2Cl_2 was added and the organic phase washed three times with dilute HCl and dried with Na_2SO_4 , and the solvent was evaporated, yielding 29 mg (90% yield) of pure (TLC one spot) $\text{Mn}^{\text{III}}(\text{ChP})\text{Cl}$. V (λ_{max} (log ϵ)): 373 (4.24), 402 (4.23), 420 (sh), 480 (4.51), 582 (3.45), and 617 nm (3.34). FABMS (*m*-nitrobenzyl alcohol matrix; $\text{M}^+ - \text{Cl}$): *m/z* 2152 (75), 2153 (100), 2154 (87), 2155 (60), 2156 (41), 2157 (20).

$\text{Cu}^{\text{II}}(\text{ChP})$. A mixture of 11.7 mg (5.57 μmol) of $\text{H}_2(\text{ChP})$, 200 mg (1 mmol) of copper(II) acetate monohydrate, and 1.56 mg (20 μmol) of pyridine was dissolved in 3 mL of a 1/1 mixture of CHCl_3 and EtOH. The solution was refluxed for 20 min, cooled, and washed three times with water, and the chloroform was evaporated, yielding 11.5 mg (>95% yield) of pure $\text{Cu}^{\text{II}}(\text{ChP})$. Vis (CH_2Cl_2 ; λ_{max} (log ϵ)): 417 (5.32), 540 nm (4.35). FABMS (*m*-nitrobenzyl alcohol matrix): *m/z* 2155 (80), 2157 (100), 2158 (83), 2159 (60), 2160 (39), 2161 (24).

$\text{Co}^{\text{II}}(\text{ChP})$. This preparation was carried out in the drybox under strictly anaerobic conditions because the $\text{Co}^{\text{II}}(\text{ChP})$ quickly autoxidizes to a Co^{III} species in the presence of air. A total of 3.2 mg (1.5 μmol) of $\text{H}_2(\text{ChP})$, 350 mg (1.5 mmol) of cobalt(II) chloride hexahydrate, and 1.5 mmol of sodium bicarbonate were mixed in 3 mL of a 1/1 mixture of benzene and ethanol. The mixture was refluxed for 1 h and cooled, and the NaHCO_3 was filtered off and washed with chloroform. The filtrate was washed twice with deaerated water, dried with Na_2SO_4 , and used as a 10-mL solution. Vis (CHCl_3 ; λ_{max} (log ϵ)): 412 (5.15), 528 nm (4.11). FABMS (*m*-nitrobenzyl alcohol matrix): *m/z* 2154 (82), 2155 (100), 2156 (88), 2157 (58), 2158 (44), 2159 (27).

Gel Permeation Chromatography. Small unilamellar DMPC vesicles with and without $\text{Cu}^{\text{II}}(\text{ChP})$ were prepared in the following manner:¹³ 10 μmol of DMPC (Sigma) and 0.1 μmol of $\text{Cu}^{\text{II}}(\text{ChP})$ were dissolved in a small amount of chloroform in a test tube. The solvent was evaporated in a stream of nitrogen, and 2 mL of distilled water was added. The mixture was then sonicated for 5 min at room temperature. Sonication was carried out using a microprobe attached to a Heat Systems MS-50 cell disruptor operated at 80% power. The vesicular solution was left standing to equilibrate at ambient temperature for 30 min and then run down a gel permeation column. The stationary phase was Sepharose 4B (Sigma) using distilled water as eluent in a 25 cm by 2 cm column. Fractions were collected at the appropriate elution volumes, and the electronic absorption was measured at 300 and 435 nm using a Cary 2130 spectrometer.

^{31}P NMR of Vesicles. Vesicles were prepared in a manner analogous to the preparation described above. Thus, 30 μmol of DMPC and 0.6 μmol (2 mol %) of $\text{Cu}^{\text{II}}(\text{ChP})$ were sonicated in the presence of 2 mL of 20% D_2O in H_2O for 5 min. ^{31}P NMR spectra were taken in 10-mm tubes on a Bruker WM-250 spectrometer at 101.26 MHz. The temperature was 26 $^\circ\text{C}$, and the spectra were averaged over 300 pulses. Peaks were referenced to aqueous phosphoric acid. A total of 2 μmol of the lanthanide shift reagent, europium(III) nitrate hexahydrate, was added as a 20 mM solution in 20% D_2O in H_2O after the vesicles had been formed.

Differential Scanning Calorimetry. Differential scanning calorimetry (DSC) experiments were carried out on multilayered vesicles. The vesicles were prepared by evaporating a 10 μmol of DMPC chloroform solution containing 2.5 mol % of $\text{Cu}^{\text{II}}(\text{ChP})$ to a thin film. An amount of 0.5 mL of phosphate buffer, pH 7.4, was added, and the preparation *only vortexed* to a milky solution. DSC's were then taken on a Perkin-Elmer DSC-4 instrument, which was calibrated on the melting point transition of cyclohexane.

Orientation of the Porphyrin Ring in the Bilayer. Orientated multilayers were formed according to a similar procedure described in the literature.^{17,23} A total of 20 μmol of DMPC and 0.2 μmol of $\text{Cu}^{\text{II}}(\text{ChP})$ were dissolved in chloroform, and the solvent was evaporated, leaving a thin film. A total of 2 mL of distilled water was added and the mixture sonicated for 1 min, forming relatively large unilamellar vesicles. The solution was then carefully spread onto a sheet of Mylar and left to dry at room temperature for 6 h. This procedure produced hydrated multilayers. The edges of the multilayer were then carefully scraped away with a razor blade, and the Mylar sheet was cut into 15 strips each 3 mm wide. The strips were bundled together and placed in a 4-mm EPR tube. EPR spectra on a Varian E-12 spectrometer were taken at various angles of the magnetic field to the plane of the Mylar strips by rotating the

magnet and/or EPR tube. Spectra were taken at 77 K: microwave power 10 mW; microwave frequency 9055 MHz; modulation frequency 100 KHz; modulation amplitude 5 G; time constant 1.0 s; scan time 8 min; receiver gain 3.2×10^3 .

Position of the Porphyrin Plane in the Vesicle Bilayer. Preparation of Tethered Imidazole Ligands. The ω -imidazolylcarboxylic acids were prepared by a modification of a literature preparation,³⁷ which entails the following reaction series: esterification of a ω -bromocarboxylic acid to form a methyl ester; nucleophilic substitution of the terminal bromide with an imidazole anion mediated by phase-transfer catalysis; hydrolysis of the ester to form the carboxylic acid product. Thus, 10 mmol of ω -bromocarboxylic acid and 1 mol of methanol were refluxed for 3 h in the presence of 0.5 mL of concentrated sulfuric acid. After cooling and addition of CHCl_3 , the solution was washed twice with water. The organic phase was dried and evaporated down to a minimum volume. The product methyl ω -bromocarboxylates were purified on a 30 cm by 2 cm silica gel column (Davisil) with chloroform as eluent, $R_f = 0.70$. Yields in all cases were >90%. The imidazole anion was prepared as sodium imidazolate by slowly adding 0.5 mol of NaH to 0.5 mol of imidazole in 300 mL of dry THF in the drybox. After 3 h (2 h addition and an additional 1 h), the mixture was filtered and the sodium imidazolate dried at the pump. Then 5 mmol of ω -bromomethylcarboxylate and 15 mmol of sodium imidazolate in 20 mL of benzene were vigorously stirred at room temperature in a 100-mL flask in the presence of Aliquot 336 for 10 h. The excess sodium imidazolate was filtered off and the benzene evaporated. A total of 100 mL of 15% NaOH was added and the mixture stirred an additional 4 h at room temperature. Hexane was added, and three phases formed. The product was in the lower aqueous phase. This phase was then acidified with concentrated HCl and the water evaporated. The solid was then extracted with boiling isopropyl alcohol for 1 h and the NaCl filtered while hot. For products of shorter alkyl chains (up to 8-imidazoyloctanoic acid hydrochloride), the product crystallized upon cooling. For products with longer alkyl chains the isopropyl alcohol was evaporated, leaving pure (TLC one spot) product. ^1H NMR (300 MHz, D_2O): (3-imidazolylpropionic acid hydrochloride) δ 8.78 (1 H, s), 7.55 (1 H, s), 7.42 (1 H, s), 4.57 (2 H, t), 3.02 (2 H, t); (5-imidazolylpentanoic acid hydrochloride) δ 8.75 (1 H, s), 7.51 (1 H, s), 7.42 (1 H, s), 4.25 (2 H, t), 2.41 (2 H, t), 1.92 (2 H, m); (6-imidazolylhexanoic acid hydrochloride) δ 8.70 (1 H, s), 7.48 (1 H, s), 7.42 (1 H, s), 4.23 (2 H, t), 2.37 (2 H, t), 1.90 (2 H, m), 1.62 (2 H, m), 1.31 (2 H, m); (8-imidazoyloctanoic acid hydrochloride) δ 8.70 (1 H, s), 7.47 (1 H, s), 7.41 (1 H, s), 4.20 (2 H, t), 2.35 (2 H, t), 2.0-1.0 (10 H, m); (10-imidazolyldecanoic acid hydrochloride) δ 8.70 (1 H, s), 7.47 (1 H, s), 7.42 (1 H, s), 4.20 (2 H, t), 2.35 (2 H, t), 2.0-1.0 (14 H, m).

EPR Spectra of Vesicles Containing $\text{Co}^{\text{II}}(\text{ChP})$ and Tethered Imidazoles. The sample preparation took place in nitrogen atmosphere to prevent significant autoxidation of $\text{Co}^{\text{II}}(\text{ChP})$ although oxygen was not strictly excluded. A total of 3 μmol of DMPC and 0.03 μmol of $\text{Co}^{\text{II}}(\text{ChP})$ in CHCl_3 were evaporated to a thin film. An amount of 0.3 mL of phosphate buffer, pH 7.4, were added and sonicated for 5 min as described above. After sonication and equilibration for 15 min, 3.0 μmol of ω -imidazolylcarboxylic acid was added by injecting 100 μL of a 30 mM solution in phosphate buffer. The vesicular solution was transferred under nitrogen to an ESR tube, sealed, and allowed to stand at room temperature for 30 min to allow for diffusion of the imidazole ligand into the vesicle. EPR spectra were taken at 77 K with a microwave power 20 mW, microwave frequency 9028 MHz, modulation frequency 100 KHz, modulation amplitude 20 G, time constant 1.0 s, scan time 8 min, and receiver gain 4×10^3 .

Oxidation Reactions in Vesicles. A typical procedure for carrying out an epoxidation reaction is as follows. A total of 10 μmol of DMPC, 1 μmol of substrate, and 0.1 μmol of $\text{Fe}^{\text{III}}(\text{ChP})\text{Cl}$ or $\text{Mn}^{\text{III}}(\text{ChP})\text{Cl}$ were dissolved in chloroform, and the solvent was evaporated under a stream of nitrogen, leaving a thin film. An amount of 4 mL of phosphate buffer was added, and the mixture was sonicated for 5 min at ambient conditions while cooling with water. The solution was left to equilibrate at 30 $^\circ\text{C}$ for 15 min and iodosylbenzene is added as a 20 mM solution in 1/1 MeOH-water. In the case of sodium periodate mediated reactions the oxidant was added as a 50 mM solution in water. After 2.5 h the reaction was quenched by addition of ether and vigorous shaking to disrupt the vesicles. The ether phase was passed over a basic alumina column to remove DMPC and the catalyst.

Analysis of reaction mixtures was performed by GC and if necessary GC-MS. For fatty acids the ether phase was concentrated and the carboxylic acids derivatized as methyl esters by addition of diazomethane. Analysis was on a 30-m Supelcowax (high-polarity) bonded phase ca-

(37) (a) Tomko, R.; Overberger, C. G. *J. Polym. Sci., Polym. Chem. Ed.* **1985**, *23*, 265. (b) Dou, H. J.-M.; Metzger, J. *Bull. Soc. Chim. Fr.* **1976**, 1861.

pillary column with a 0.32-mm i.d. and a 0.25- μm coating. The column temperature was isothermal at 210 °C with detection by FID at 280 °C. Temperature at the injector port was 230 °C. Retention times were as follows: methyl linoleate, 8.04 min; methyl oleate, methyl vaccenate, and methyl petroselenate, 7.93 min; 9,12(*E,E*)-methyl octadecadienate, 8.05 min; 9(*Z*)-methyl 12,13-epoxyoctadecenoate, 20.72 min; 12(*Z*)-methyl 9,10-epoxyoctadecenoate, 21.08 min; 9(*E*)-methyl 12,13-epoxyoctadecenoate, 19.27 min; 12(*Z*)-methyl 9,10-epoxyoctadecenoate, 19.45 min; 6,7-methyl epoxystearate, 19.80 min; methyl 9,10-epoxystearate, 20.53 min; methyl 11,12-epoxystearate, 20.90 min. Steroids were analyzed on a 30-m SPB-1 (nonpolar) bonded phase capillary column with a 0.32-mm i.d. and a 0.25- μm coating. The column temperature was isothermal at 260 °C. Retention times were as follows: cholesterol, 17.5 min; 5 α ,6 α -epoxycholesterol, 22.5 min; 5 β ,6 β -epoxycholesterol, 23.4 min; 25-hydroxycholesterol, 26.4 min; stigmasterol, 22.7 min; 22,23-epoxy-

stigmasterol, 26.2 min; fucosterol, 25.3 min; 24,28-epoxyfucosterol, 33.4 min. Desmosterol and its reaction products were analyzed as 3 β -trimethylsilyl ethers after derivatization with chlorotrimethylsilane and hexamethyldisilazane: desmosterol, 21.8 min; 5 β ,6 β -epoxydesmosterol, 28.6 min; 5 α ,6 α -epoxydesmosterol, 30.5 min; 24,25-epoxydesmosterol, 29.1 min. 25-Hydroxycholesterol was also identified by GC-MS and compared to an authentic sample (Research Plus). The retention time was 26.4 min. MS: *m/z* 402 (24), 384 (100), 369 (47), 367 (13), 351 (36), 300 (28), 299 (33), 273 (38), 271 (69), and lower *m/z* steroidal clusters.

Acknowledgment. Support for the research by the National Science Foundation (Grant CHE-87-06310) is gratefully acknowledged. The NSF and NIH provided funds for the purchase of the high-resolution FABMS-GC.

Quantification of Singlet Oxygen Generated by Thermolysis of 3,3'-(1,4-Naphthylidene)dipropionate. Monomol and Dimol Photoemission and the Effects of 1,4-Diazabicyclo[2.2.2]octane

Paolo Di Mascio and Helmut Sies*

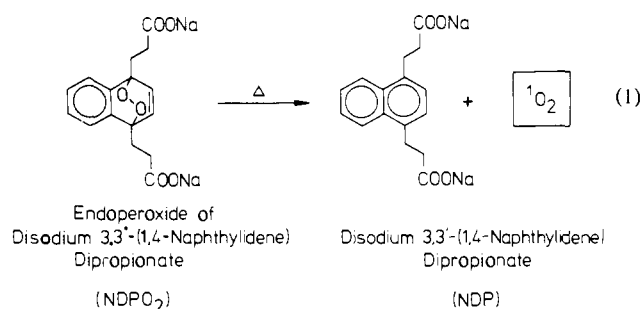
Contribution from the Institut für Physiologische Chemie I, Universität Düsseldorf, Moorenstr. 5, D-4000 Düsseldorf, FRG. Received March 25, 1988

Abstract: Singlet oxygen arising from the thermal decomposition of the water-soluble endoperoxide of 3,3'-(1,4-naphthylidene)dipropionate (NDPO₂) or from hypochlorite/H₂O₂ was detected. Direct measurements of light emission due to the chemiluminescent transition of O₂ (¹Δ_g) to the triplet ground state was monitored (a) by monomol emission in the near-infrared (1270 nm) with a liquid nitrogen cooled germanium diode and (b) by dimol emission in the visible spectral region (634 and 703 nm) with a red-sensitive photomultiplier and photon counting. Chemical trapping of ¹O₂ generated by NDPO₂ or by hypochlorite/H₂O₂ was used for quantification with the anthracene-9,10-diyldiethyl disulfate (EAS), yielding the endoperoxide (EASO₂) as the specific oxidation product. The β value for EASO₂ was calculated to be 7.7×10^{-3} M and 8×10^{-3} M when ¹O₂ was generated by NDPO₂ or hypochlorite/H₂O₂, respectively. Due to the enhancement of the lifetime of ¹O₂, the β values were lower in D₂O. The yields of ¹O₂ were measured, showing that one-half of the O₂ liberated by thermolysis of NDPO₂ was in the singlet state, whereas the yield for hypochlorite/H₂O₂ was near unity. The addition of 1,4-diazabicyclo[2.2.2]octane (DABCO) increased dimol emission with a concomitant decrease of monomol light emission, but left the yield of EASO₂ unchanged. Similar results were obtained with hypochlorite/H₂O₂. A calibration of the photoemission was performed, based on the ¹O₂ yield of NDPO₂ thermodissociation.

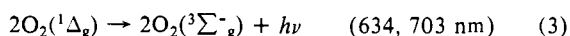
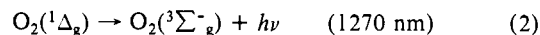
1. Introduction

Several methods have been described for the generation of singlet molecular oxygen (¹O₂), e.g. photosensitization, chemical oxidants, and microwave discharge. Chemical sources of ¹O₂ include aromatic endoperoxides that liberate ¹O₂ by thermolysis.¹⁻⁴ Such compounds can be individually designed to exhibit desired solubility characteristics and thermodissociation temperature. Aromatic endoperoxides such as alkyl- and aryl-substituted naphthalenes decompose thermally in solution into the parent hydrocarbon and molecular oxygen.⁴⁻⁷ We studied the thermal decomposition of the water-soluble disodium salt 3,3'-(1,4-naphthylidene)dipropionate (NDPO₂),⁴ as shown in reaction 1.

We describe the quantification of ¹O₂ generated by the thermal decomposition of NDPO₂ using a chemical trap, the water-soluble sodium salt of anthracene-9,10-diyldiethyl disulfate (EAS), and



the employment of sodium azide as ¹O₂ quencher as well as the detection of monomol (reaction 2) and dimol (reaction 3) emission.



Further, we report new observations on the effect of DABCO on monomol and dimol emission, and we show the calibration of the photoemission signals. The effects are compared to those obtained with hypochlorite/H₂O₂.

2. Experimental Section

2.1. Reagents. Reagents were purchased from the following sources: 1,4-dimethylnaphthalene, benzoyl peroxide, azodiisobutyronitrile, N-

(1) Foote, C. S.; Shook, F. C.; Abakerli, R. A. *Methods Enzymol.* **1984**, *105*, 36-47.

(2) Wasserman, H. H.; Scheffer, J. R. *J. Am. Chem. Soc.* **1967**, *89*, 3073.

(3) Turro, N. J.; Chow, M. F.; Rigaudy, J. *J. Am. Chem. Soc.* **1981**, *103*, 7218-7224.

(4) Aubry, J. M. *J. Am. Chem. Soc.* **1985**, *107*, 5844-5849.

(5) Saito, I.; Matsuura, T.; Inoue, K. *J. Am. Chem. Soc.* **1983**, *105*, 3200-3206.

(6) Chou, P. T.; Frei, H. *Chem. Phys. Lett.* **1985**, *122*, 87-92.

(7) Saito, I.; Nagata, R.; Nakagawa, H.; Momiyama, H.; Matsuura, T.; Inoue, K. *Free Radical Res. Commun.* **1986**, *2*, 327-336.